DOI: 10.1534/genetics.109.110031

# Sen1p Performs Two Genetically Separable Functions in Transcription and Processing of U5 Small Nuclear RNA in *Saccharomyces cerevisiae*

**Jonathan S. Finkel, Karen Chinchilla, Doris Ursic and Michael R. Culbertson**[1]

*Laboratories of Genetics and Molecular Biology, University of Wisconsin, Madison, Wisconsin 53706*

Manuscript received September 24, 2009
Accepted for publication October 23, 2009

ABSTRACT

The *Saccharomyces cerevisiae SEN1* gene codes for a nuclear-localized superfamily I helicase. *SEN1* is an ortholog of human *SETX* (senataxin), which has been implicated in the neurological disorders ataxia-ocular apraxia type 2 and juvenile amyotrophic lateral sclerosis. Pleiotropic phenotypes conferred by *sen1* mutations suggest that Sen1p affects multiple steps in gene expression. Sen1p is embedded in a protein–protein interaction network involving direct binding to multiple partners. To test whether the interactions occur independently or in a dependent sequence, we examined interactions with the RNA polymerase II subunit Rpb1p, which is required for transcription, and Rnt1p, which is required for 3′-end maturation of many noncoding RNAs. Mutations were identified that impair one of the two interactions without impairing the other interaction. The effects of the mutants on the synthesis of U5 small nuclear RNA were analyzed. Two defects were observed, one in transcription termination and one in 3′-end maturation. Impairment of the Sen1p–Rpb1p interaction resulted in a termination defect. Impairment of the Sen1p–Rnt1p interaction resulted in a processing defect. The results suggest that the Sen1p–Rpb1p and Sen1p–Rnt1p interactions occur independently of each other and serve genetically separable purposes in targeting Sen1p to function in two temporally overlapping steps in gene expression.

PROTEIN–protein interaction networks contribute tfhe underlying basis for phenotypic pleiotropy. In *Saccharomyces cerevisiae*, global studies suggest that each protein interacts on average with five other proteins (Grigoriev 2003), leading to a complex network of interactions involving at least 16,000 individual protein–protein interactions that influence the functions of wild-type proteins and the phenotypes of mutants. The essential *S. cerevisiae SEN1* gene codes for a nuclear-localized nucleic acid helicase (DeMarini *et al.* 1992) that is embedded in a complex network of protein–protein interactions (Ursic *et al.* 2004). Furthermore, mutations in *SEN1* confer pleiotropic phenotypes, including defects in transcription termination, RNA processing, and DNA repair (Steinmetz and Brow 1996, 1998; Rasmussen and Culbertson 1998; Steinmetz *et al.* 2001, 2006; Ursic *et al.* 2004). The study of *SEN1* therefore provides a useful paradigm to examine the impact of protein–protein interactions on mutant phenotypes and function.

Mutations in human *SETX* (senataxin), the ortholog of yeast *SEN1*, cause two clinically distinct neurological diseases, ataxia-ocular apraxia 2 and juvenile amyotrophic lateral sclerosis (Chen *et al.* 2004, 2006; Moreira *et al.* 2004; Duquette *et al.* 2005; Suraweera *et al.* 2007; Suraweera *et al.* 2009). The yeast and human proteins are strikingly similar in their organization. Some of the human mutations cause changes in the ATP-helicase domain, whereas others cause changes in the N-terminal region where protein-binding domains reside. Some of the clinical differences might be caused by mutations that differentially affect the function of senataxin by disrupting different protein–protein interactions.

Sen1p interacts with the C-terminal domain of Rpb1p, the largest subunit of RNA polymerase II (RNAP II) (Myer and Young 1998); with Rad2p, a single-strand DNA endonuclease required for DNA repair (Habraken *et al.* 1993; Prakash and Prakash 2000); with Rnt1p, a double-strand RNA cleavage enzyme involved in 5′- or 3′-end processing (Elela *et al.* 1996; Chanfreau *et al.* 1997; Lamontagne *et al.* 2000); and with SmD3p (Fromont-Racine *et al.* 1997), a subunit of the heteroheptameric Sm complex that assembles small nuclear RNAs (snRNAs) into ribonucleoprotein particles required for pre-mRNA splicing (Roy *et al.* 1995; Kambach *et al.* 1999; Zhang *et al.* 2001). Recently, it was shown that Sen1p interacts with Glc7p, a protein phosphatase subunit of the cleavage/polyadenylation factor, and with Nab3p, a RNA-binding protein that interacts with other proteins involved in transcription termination of noncoding RNAs (Conrad *et al.* 2000; Nedea *et al.* 2008).

RNA processing, ribonucleoprotein assembly, and transcription-coupled DNA repair occur concomitantly with transcription (Komarnitsky *et al.* 2000; Maniatis

[1]*Corresponding author:* Robert M. Bock Labs, 1525 Linden Dr., University of Wisconsin, Madison, WI 53706.
E-mail: mrculber@wisc.edu

and Reed 2002; Neugebauer 2002; Hanawalt and Spivak 2008), suggesting a complex interplay between protein–protein interactions that potentially orchestrate cotranscriptional pathways. The interactions of Sen1p with proteins involved in transcription, processing, and repair might occur independently of each other or they might occur in a dependent sequence of interactions.

To begin assessing the relationships between the different Sen1p protein–protein interactions, we analyzed the effects of *sen1* mutations on the expression of *SNR7,* which codes for U5 snRNA. *SNR7* serves as a diagnostic indicator of the relationship between Sen1p protein–protein interactions and Sen1p function because previous studies based on depletion assays suggested a role for *SEN1* in U5 RNA 3′-end processing (Ursic *et al.* 2004). Other reports indicated that Sen1p plays a role in the transcription termination of noncoding RNAs (Steinmetz and Brow 1996, 1998; Rasmussen and Culbertson 1998; Steinmetz *et al.* 2001, 2006). Furthermore, the Sen1p-interacting partners Rpb1p and Rnt1p are required for U5 snRNA transcription and maturation, respectively (Myer and Young 1998).

The U5 snRNA transcript matures through a branched pathway leading to the production of two functional end products, U5L (214 nucleotides) and U5S (180 nucleotides) (Patterson and Guthrie 1987; Chanfreau *et al.* 1997) (see Figure 1B). During cotranscriptional maturation, Rnt1p cleaves at two locations in a stem–loop structure leading to accumulation of U5L-3′ RNA (240 nucleotides) and U5-3′a RNA (270 nucleotides). The exosome removes 3′ nucleotides from each of the cleavage products to form mature U5L and U5S RNA, respectively (Allmang *et al.* 1999). Despite this, a deletion of *RNT1* affects only synthesis of U5L, indicating that a Rnt1-independent bypass pathway allows for U5S RNA synthesis in the absence of Rnt1p cleavage. Sen1p and Rnt1p are required for production of U5L RNA but not for U5S RNA (Ursic *et al.* 2004).

To distinguish whether the interactions with Rpb1p and Rnt1p have a dependent or independent relationship, *sen1* mutations that impair one interaction without impairing the other interaction were identified. The phenotypes were assessed to determine their effects on *SNR7* expression. Two defects were observed, one in transcription termination and one in 3′ processing. The genetic data support a model in which the interactions occur independently of each other.

## MATERIALS AND METHODS

**Strains, genetic methods, and plasmids:** Strains carrying *sen1-1* were derived from FWY1 (*MAT***a** *ura3-52 leu2-3, −112 pep4-3 trp1 sen1-1*) (Ursic *et al.* 2004); *sen1-2* from DDY86 (*MATα ade2-101 his3-200 lys2-801 trp1-Δ1 ura3-52 leu2-Δ1::sen1-2*) (DeMarini *et al.* 1992); *sen1-K128E* from JFY41 (*MAT***a** *leu2Δ ura3Δ his3Δ1 trp1Δ sen1-K128E*) (this study); *sen1-R302W* from DUY1513 (*MAT***a** *leu2Δ ura3Δ his3Δ1 met15Δ sen1-R302W*) (this study); *rrp6Δ* from BY4742 (*MATα his3Δ1 leu2Δ lys2Δ ura3Δ rrp6Δ::KanMX4*) (Open Biosystems); *rnt1Δ* from JFY5 (*MATα ade2-101 his3-200 leu2-Δ1::sen1-2 HIS3:pet56:rnt1*) (Ursic *et al.* 2004); and *mtr4-1* from *YSL402* (*MAT***a** *ura3-52 lys2-801 pep4::HIS3 prb1-Δ1.6R mtr4-1*) (Liang *et al.* 1996). Isogenic sets of strains were created by two-step gene replacement (Boeke *et al.* 1984). Standard yeast mating and dissection techniques were used to construct double mutants. Growth media were described previously (Ursic *et al.* 2004). Gene deletions were constructed using the PCR-based gene disruption method (Wach *et al.* 1994).

All strains were grown at 30°. Strains carrying *sen1-K128E* and *sen1-R302W* grow at normal rates. Strains carrying *sen1-2* in single copy are viable but grow at a reduced rate. Strains carrying *sen1-1* are temperature sensitive for growth. Thirty degrees is permissive for growth, but the changes in levels of accumulation of U5-related RNAs at 30° resemble the changes observed at a nonpermissive temperature of 37°.

The plasmids pU5mt and pU5wt contain DNA starting 500 nucleotides upstream of *SNR7* and ending 500 nucleotides downstream of the *TOS2* open reading frame (ORF). pU5mt contains GAAA in the stem-loop recognized by Rnt1p in place of AGUC in pU5wt (see Figure 4A). pJF89 contains the same DNA insert as in pU5wt except that the *TOS2* ORF is replaced with the *Escherichia coli lacZ* ORF. Plasmids were introduced into strains by lithium acetate transformation (Gietz and Woods 2002).

**RNA methods:** Methods for RNA isolation and Northern blotting were described previously (Ursic *et al.* 2004). RNAs (10 μg) were fractionated on 2% agarose or 6% acrylamide:8 M urea (29:1) gels, transferred to GeneScreen Plus membranes (NEN Life Science Products), and crosslinked using a UV Stratalinker 2400 (Stratagene). Probes were labeled using T4 polynucleotide kinase (Pharmacia) in the presence of [γ-$^{32}$P]ATP (Amersham). Riboprobes used in Figure 6B were prepared using an *in vitro* transcription kit (Promega) in the presence of [α-$^{32}$P]CTP and [α-$^{32}$P]UTP (3000 Ci/mmol) (Perkin-Elmer). Band intensities on the Northern blots were quantitated using a Typhoon 9200 Variable Mode Imager (Amersham Biosciences). Oligonucleotide probes (Thermo Scientific) used for Northern blotting to map the U5-3′b 3′-end were as follows: U5A (CGCCCTCCTTACTCATTG), U5D (TAATCCATCTTCGGTAAATAG), U5E (GCATTGCTGTCT GAGTTTG), and TOS2 (TTATACATGTACATTCTCG).

The rate of *TOS2* mRNA decay was determined by measuring the temporal decline in mRNA by Northern blotting following transcription inhibition using 10 μg/ml thiolutin (Pfizer) (Guan *et al.* 2006). *SCR1* RNA was monitored as a loading control. SigmaPlot was used to evaluate decay data using the following exponential decay formula: $y = a \times \exp(-b \times x)$. Estimations of $b$, designated as B, and corresponding standard errors, were used to calculate standard error [$t_{1/2} = \log(2)/B$]. $t_{1/2} \pm \mathrm{SE}(t_{1/2})$ was calculated as [$\log(2)/(B + \mathrm{SE}(B))$, $\log(2)/(B\text{-}\mathrm{SE}(B))$].

The relative levels of U5-related RNAs detected by Northern blotting were determined as follows. U5S RNA was used as an internal standard in each gel lane because U5S levels are not affected by mutations in *SEN1* or *RNT1* (Chanfreau *et al.* 1997, 1998; Ursic *et al.* 2004). U5-related RNAs were named as described previously (Chanfreau *et al.* 1997). The relative levels of U5L-3′ RNA, U5-3′b RNA, and the sum of the RNAs ranging in size from 271 to 960 nucleotides (designated RNA271–960) were measured by calculating the band intensities of the RNAs divided by the band intensity corresponding to U5S RNA in the same lane. Fold changes were calculated by dividing the ratios in mutant strains by the ratio in the corresponding wild-type strain.

**Protein and immunological methods:** β-Galactosidase activity was measured as described previously (Stahl *et al.* 1995). Immunoprecipitation (IP) and Western blotting were

described previously (Ursic *et al.* 2004). Primary antibodies that recognize epitope-tagged proteins were as follows: mouse monoclonal anti-HA antibody (clone HA-7, Sigma) recognizes Rpb1p-HA; mouse monoclonal anti-cMyc antibody (clone 9E10, Sigma) recognizes cMyc-Sen1p, cMyc-sen1-K128Ep, and cMyc-sen1-R302W; and rabbit anti-tandem affinity purification (TAP) antibody (Thermo Scientific) recognizes Rnt1p-TAP, Sen1p-TAP, sen1-K128Ep-TAP, and sen1-R302Wp-TAP. Membranes for Western blotting were probed with anti-mouse or anti-rabbit peroxidase-conjugated antibodies (Thermo Fisher Scientific). Protein bands were visualized by chemiluminescence (SuperSignal West Pico chemiluminescent substrate, Thermo Fisher Scientific) and quantified using a Typhoon 9200 Variable Mode Imager (Amersham Biosciences). For IP experiments, 10 μg/ml RNase A (Sigma) was added to pre-IP lysates. The relative amount of protein that copurified with an immunoprecipitated protein was determined by comparing the ratio of the band intensity of the immunoprecipitated protein to the band intensity of the copurifying protein detected by Western blotting of IP lysates. The effects of *sen1* mutations on the extent of copurification were determined by calculating the ratio of the band intensities of the immunoprecipitated and co-immunoprecipitated proteins in the mutant divided by the ratio of the band intensities in wild type.

## RESULTS

**Sen1p affects two steps in the expression of *SNR7*:** Two alleles of *SEN1* that affect the expression of genes for noncoding RNAs were described previously (Figure 1A) (DeMarini *et al.* 1992). The *sen1-1* mutation (G1747D) is located in a conserved motif in the ATP-helicase region of *SEN1*. On the basis of its location, *sen1-1* most likely impairs helicase activity. The *sen1-2* mutation is a partial deletion producing a stable, truncated protein lacking the first 975 amino acids of Sen1p. The deletion removes binding domains required for interaction with the RNase III cleavage enzyme Rnt1p and the largest RNA polymerase II subunit, Rpb1p (Ursic *et al.* 2004). Depletion of the *sen1-2* protein causes a time-dependent accumulation of U5L-3′ RNA, the product of Rnt1p cleavage, at the expense of mature U5L RNA (Ursic *et al.* 2004). This establishes that elevated accumulation of U5L-3′ RNA is a diagnostic indicator of a Sen1-mediated processing defect.

Using a U5-specific probe, we examined the steady-state levels of U5-related RNAs by Northern blotting of RNA from strains carrying the *sen1-1*, *sen1-2*, and/or *rnt1*Δ mutations (Figure 1B). When the relative levels of U5L-3′ RNA were analyzed (Figure 1C), the *sen1-1* mutation caused a 2.9 ± 0.2-fold increase in accumulation, whereas the *sen1-2* mutation caused a 2.5 ± 0.2-fold increase. The strains carrying *rnt1*Δ caused a significant reduction in the level of U5L-3′ RNA since this RNA is the product of Rnt1p cleavage. A small amount of U5L-3′ RNA can still be detected in *rnt1*Δ strains, presumably due to inefficient degradation of a longer precursor by the exosome, which may stall at the stem-loop recognized by Rnt1p. These results are consistent with data showing that *sen1-2* causes a time-dependent increase in the accumulation of U5L-3′ at the expense of U5L RNA but with no effect on U5S accumulation (Ursic *et al.* 2004).

The longest detectable U5-related RNA, U5-3′b, is ~960 nucleotides in length (Figure 1B; see below). This RNA accumulated to a 2.8 ± 0.8-fold higher level in a *sen1-1* strain (Figure 1D). However, excess accumulation of U5-3′b RNA was not observed in a *sen1-2* strain. When double mutants were analyzed, U5-3′b RNA accumulated in excess in both *sen1-1 rnt1*Δ and *sen1-2 rnt1*Δ strains (8.9 ± 1.3-fold and 9.3 ± 1.1-fold, respectively). These results suggest that Rnt1p cleavage limits the accumulation of U5-3′b RNA and partially or completely masks the effects of *sen1-1* and *sen1-2* on accumulation. Overall, the results show that *sen1-1* and *sen1-2* affect the accumulation of two RNAs, U5L-3′ and U5-3′b. Furthermore, both the N-terminal and helicase regions of Sen1p are required for efficient expression of *SNR7*.

The distance between the 3′-end of U5L-3′ RNA and the beginning of the downstream *TOS2* ORF is 466 nucleotides. The estimated length of U5-3′b RNA suggested that it might extend into the downstream *TOS2* gene and could be a readthrough transcript. To test this possibility, the 3′-end of U5-3′b RNA was approximated by Northern blotting of RNA from a *sen1-1 rnt1*Δ strain using probes complementary to sequences spanning the region from the *SNR7* gene to the end of the *TOS2* ORF (Figure 1E). Probe U5A, which is complementary to sequences near the 3′-end of mature U5L RNA, hybridized to U5-3′b RNA, whereas the *TOS2* probe detected *TOS2* mRNA but not U5-3′b RNA. When the two probes were mixed, both RNAs were detected, verifying that RNAs of different sizes were detected with U5-3′b RNA being the smaller of the two. The approximate 3′-end of U5-3′b RNA was located by observing that probe U5D (3′-end at nucleotide 950) hybridized to U5-3′b and *TOS2* RNA, whereas probe U5E (5′-end at nucleotide 970) hybridized only to *TOS2* mRNA.

The 3′-end of U5-3′b RNA is therefore likely to be located at a position between 940 and 980 nucleotides from the beginning of transcription of *SNR7*. Since the 3′-end is located between 260 and 300 nucleotides downstream of the beginning of the *TOS2* ORF, U5-3′b RNA is most likely a readthrough transcript that accumulates in *sen1-1 rnt1*Δ strains. Overall, these results suggest that *sen1-1* and *sen1-2* affect accumulation of two RNAs: an intermediate in RNA processing and a readthrough transcript presumed to result from impaired termination of transcription.

**Impact of Sen1p–Rnt1p and Sen1p–Rpb1p interactions on Sen1p function:** Mutations in *SEN1* that reduce the efficacy of specific protein–protein interactions might provide insights into the role of the interactions in Sen1p function. To pursue the genetic approach, the boundaries of the binding domains for interaction with Rnt1p and Rpb1p were approximated using polypeptide fragments of Sen1p in two-hybrid studies (Figure 1A). Direct physical interactions of Sen1p with Rnt1p and Rpb1p

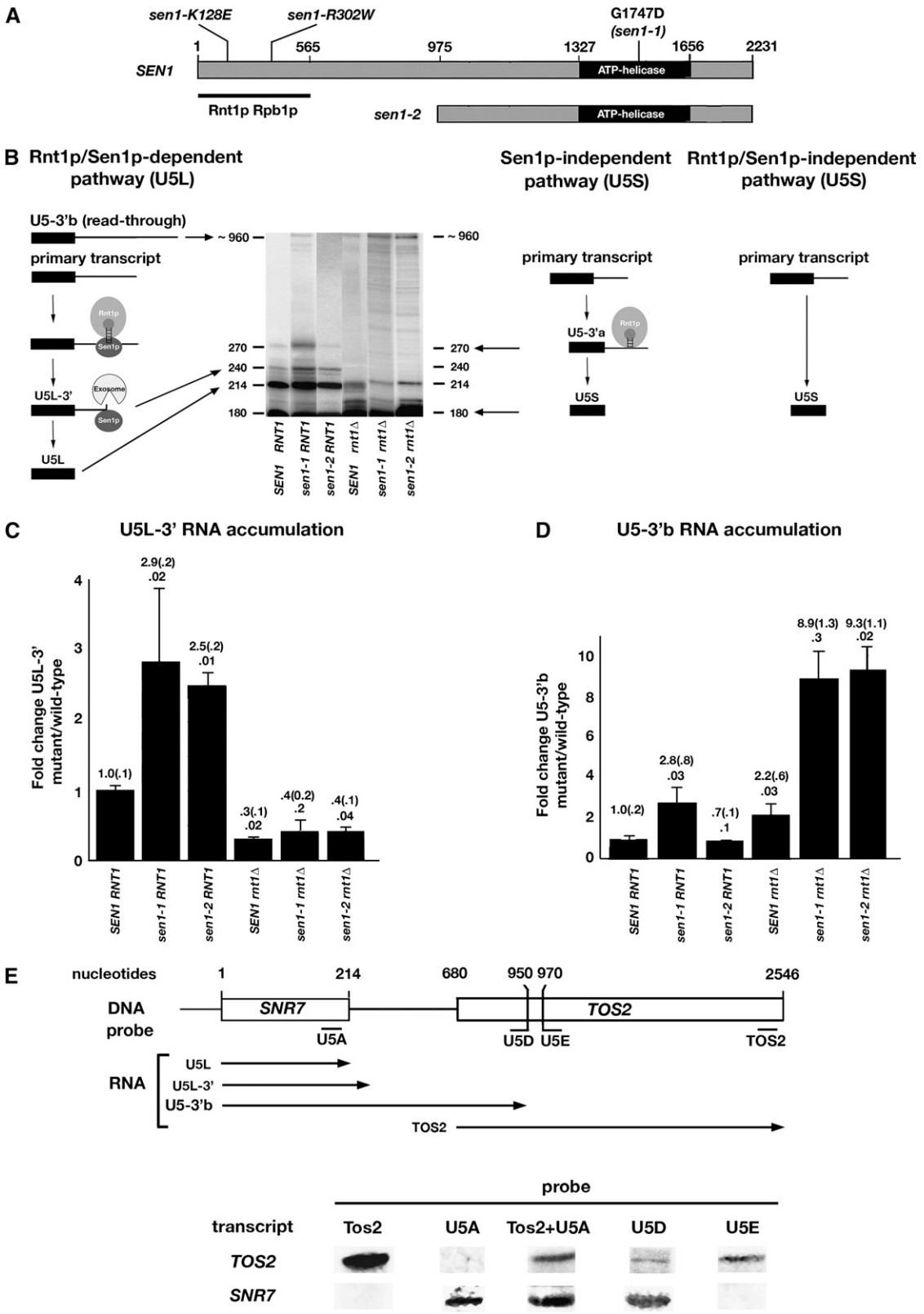


Figure 1.—Sen1p mutations and interactions. (A) Schematic of Sen1p showing the locations of the interaction domains for Rbp1p and Rnt1p (Ursic *et al.* 2004; Nedea *et al.* 2008). *Sen1* alleles that affect interactions (*sen1-K128E*, *sen1-R302W*, *sen1-2*) or function (*sen1-1*) are shown. Numbers refer to amino acids. (B) Alternative pathways for U5 snRNA synthesis. RNAs are named as previously described (Elela *et al.* 1996; Chanfreau *et al.* 1997; Lamontagne *et al.* 2000). The length of the primary transcript is unknown. Shown is a representative Northern blot in which RNAs were fractionated by PAGE and detected using a complementary probe spanning nucleotides 1–320 of the *SNR7* gene, which codes for U5 RNA (materials and methods). (C) Effects of *sen1-1* and *sen1-2* on the relative accumulation of U5L-3′ RNA, an intermediate in 3′-end processing. (D) The effects of *sen1-1* and

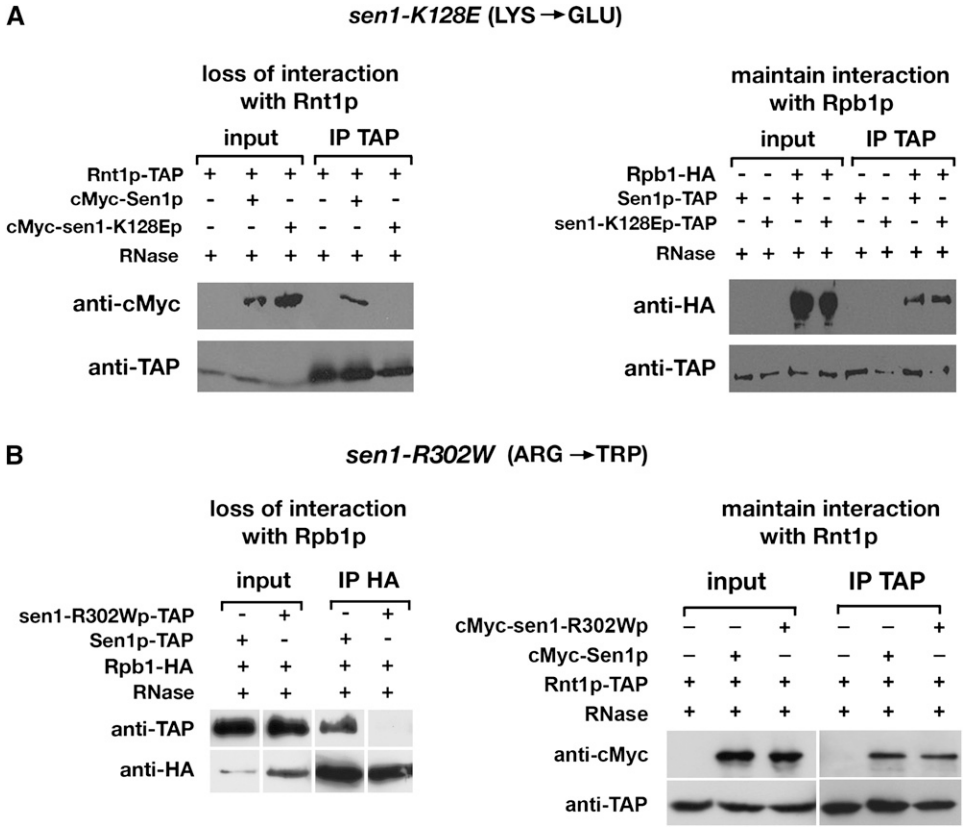


FIGURE 2.—Effects of amino acid substitutions on the interactions of Sen1p with Rnt1p and Rpb1p. (A) *sen1-K128E* impairs the interaction of Sen1p with Rnt1p (left) but does not affect the interaction with Rpb1p (right). Proteins were immunoprecipitated from cell lysates in the presence of 10 μg/ml RNase A using anti-TAP antibodies. The pre- and post-IP lysates were assayed by Western blotting using anti-cMyc and anti-TAP antibodies (MATERIALS AND METHODS). (B) *sen1-R302W* impairs the interaction of Sen1p with Rpb1p (left) but does not affect the interaction with Rnt1p (right). Experiments were performed as described in A except that the pre- and post-IP lysates were assayed by Western blotting using anti-HA and anti-TAP antibodies.

were previously demonstrated using two-hybrid and co-IP analyses (URSIC *et al.* 2004). Phylogenetic comparisons of sequences within the domains were used to identify conserved sites potentially important for each interaction. By screening a collection of candidate mutations for their effects in two-hybrid tests, it was found that *sen1-K128E* and *sen1-R302W* impaired the Sen1p–Rnt1p and Sen1p–Rpb1p interactions, respectively.

The alleles were examined by co-IP of proteins in native complexes (Figure 2). To examine *sen1-K128E*, protein extracts from strains expressing epitope-tagged cMyc-Sen1p or cMyc-sen1-K128Ep with Rnt1p-TAP were analyzed (Figure 2A, left). Proteins were bound to anti-TAP antibodies, eluted from beads, and analyzed by Western blotting using anti-TAP and anti-cMyc antibodies. The results indicate that wild-type Sen1p copurified with wild-type Rnt1p. However, the *K128E* mutation abolished the ability of the proteins to copurify. To test whether the loss of copurification was specific for the interaction with Rnt1p, protein extracts from strains expressing Sen1-TAP or sen1-K128E-TAP and Rpb1p-HA were analyzed (Figure 2A, right). Western blotting of the IP lysates shows that the *K128E* mutation had no discernible effect on the extent of copurification of Sen1p and Rpb1p.

Similar experiments were performed to analyze the effects of *sen1-R302W*. Protein extracts from strains expressing Sen1p-TAP or sen1-R302W-TAP with Rpb1p-HA were examined by co-IP of proteins bound to anti-HA antibodies (Figure 2B, left). Western blotting of the IP lysates indicated that wild-type Sen1p copurified with Rpb1p, but sen1-R302Wp failed to copurify. However, when protein extracts from strains expressing cMyc-Sen1p or cMyc-sen1-R302Wp with Rnt1p-TAP were analyzed (Figure 2B, right), the R302W mutation had no discernible effect on copurification.

Although the results described above do not necessarily indicate that protein–protein binding is completely abolished, it was reasoned that the interactions might be sufficiently impaired that the mutations would have unique phenotypic effects on Sen1p function. To assess the functional consequences, strains expressing chromosomally integrated *sen1-K128E* and *sen1-R302W* alleles were analyzed by Northern blotting with a U5-specific probe (Figure 3A). The *K128E* mutation caused

*sen1-2* on the relative accumulation of U5-3′b RNA, a readthrough transcript. Fold changes are indicated with standard error in parentheses. *P*-values are indicated below the fold changes. Methods of quantitation are described in MATERIALS AND METHODS. (E) To delimit the location of the 3′-end of U5-3′b RNA, PAGE-fractionated RNAs from a *sen1-1 rnt1*Δ strain were analyzed by Northern blotting with probes complementary to segments as shown.

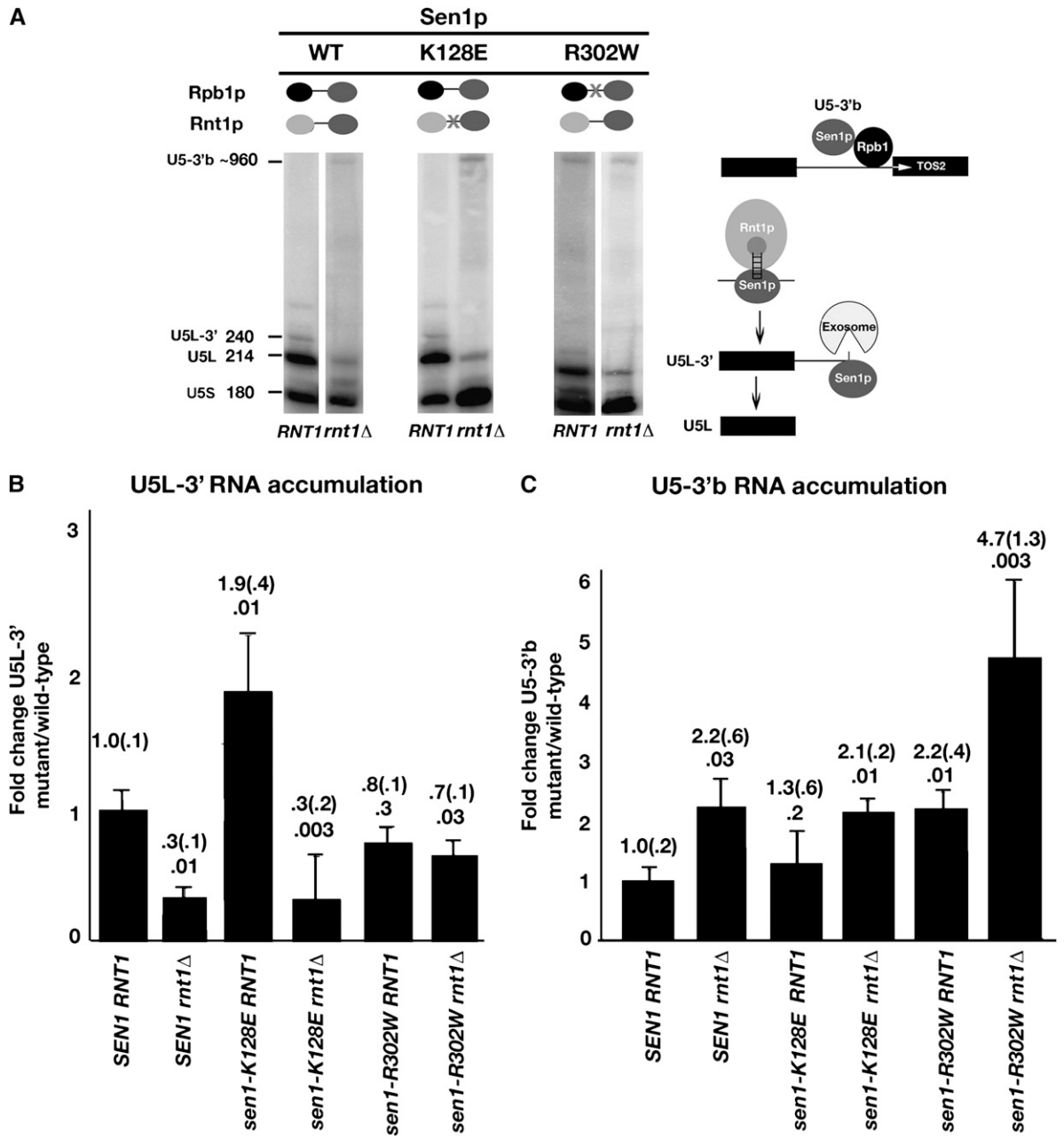


FIGURE 3.—Effects of *sen1-K128E* and *sen1-R302W* on U5 snRNA synthesis. (A) A representative Northern blot in which RNAs from *RNT1* and *rnt1*Δ strains carrying alleles of *SEN1* were analyzed as described in the Figure 1 legend. The effects of *sen1-K128E* and *sen1-R302W* on the relative accumulation of the processing intermediate U5L-3′ RNA (B) and the readthrough RNA U5-3′b (C) were quantitated as described in MATERIALS AND METHODS. Fold changes are indicated with the standard error in parentheses. *P*-values are indicated below the fold changes.

a 1.9 ± 0.4-fold increase in the relative accumulation of U5L-3′ RNA, the product of Rnt1p cleavage (Figure 3B). The increase was abolished in a *sen1-K128E rnt1*Δ double mutant. In a *sen1-K128E RNT1* strain, there was no significant effect on the relative accumulation of U5-3′b RNA, the readthrough product (Figure 3C). In the *sen1-K128E rnt1*Δ double mutant, a 2.1 ± 0.2-fold increase was observed. This was similar to that observed for a *SEN1 rnt1*Δ strain, indicating that the increase is attributable to *rnt1*Δ and not to *sen1-K128E*.

The *R302W* mutation had no effect on the relative accumulation of the U5L-3′ RNA-processing intermediate in *RNT1* or *rnt1*Δ strains (Figure 3B). When the accumulation of the U5-3′b readthrough RNA was examined, *sen1-R302W* caused a 2.2 ± 0.4-fold increase in a *RNT1* strain (Figure 3C). A similar increase of 2.2 ± 0.6-fold was observed in a *SEN1 rnt1*Δ double mutant, and a 4.7 ± 1.3-fold increase was observed in a *sen1-R302W rnt1*Δ double mutant (Figure 3C). The synthetic phenotype of the double mutant suggests that the

R302W amino acid substitution specifically affects accumulation of the readthrough RNA. Overall, the results suggest that *sen1-R302W* causes a defect in transcription termination without affecting 3′-end processing.

**Functional relationship between Sen1p and the exosome:** Since the product rather than the substrate of Rnt1p cleavage accumulates in strains carrying *sen1-2* and *sen1-K128E*, the Sen1p–Rnt1p interaction is not functionally related to cleavage itself. We reasoned that the interaction could leave Sen1p, a 5′–3′ helicase, bound to the 3′-end of the RNA cleavage product. From that location, Sen1p could unwind the stem-loop (Figure 4A) and separate the cleaved RNAs. This might allow more efficient access for the exosome, which processes the 3′-end of the Rnt1p cleavage product in conjunction with the Trf4p/Air2p/Mtr4p polyadenylation complex (TRAMP) (Liang *et al.* 1996; Lacava *et al.* 2005; Milligan *et al.* 2005). To test potential relationships of Sen1p with the exosome and TRAMP, we analyzed the phenotypes of *sen1-K128E* combined with *rrp6*Δ, a viable deletion of *RRP6*, which codes for an exosomal subunit required in U5 snRNA processing (Allmang *et al.* 1999), and *mtr4-1*, an allele of *MTR4*, which codes for a 3′–5′ helicase subunit of TRAMP (Liang *et al.* 1996).

Single-mutant strains carrying *sen1-K128E* or *rrp6*Δ were compared with a *sen1-K128E rrp6*Δ double mutant by assaying effects on the accumulation of two sets of RNAs: the processing intermediate U5L-3′ RNA and the sum of RNAs in the 271–960 nucleotide size range, which includes the U5-3′b readthrough RNA. For the latter, we settled on the broader range of larger RNAs to include intermediates in exosomal degradation of the readthrough transcript.

A synthetic phenotype was observed for U5L-3′ RNA accumulation in the *K128E rrp6*Δ double mutant (Figure 4B). In the single mutants, the *sen1-K128E* mutation caused a 2.0 ± 0.3-fold increase in the relative accumulation of U5L-3′ RNA, whereas *rrp6*Δ caused a 2.3 ± 0.4-fold increase. However, a 4.6 ± 1.6-fold increase was observed in the double mutant, which is significantly higher than in either single mutant. When RNAs in the 271–960 nucleotide size range were examined, the *sen1-K128E* and *rrp6*Δ single mutants had no significant effect on relative accumulation. In the double mutant, no synthetic increase was observed. If anything, accumulation was marginally reduced, indicating that the synthetic interaction is restricted to effects on the U5L-3′ processing intermediate.

Similar experiments were performed to compare *sen1-K128E* and *mtr4-1* single mutants with a *sen1-K128E mtr4-1* double mutant (Figure 4C). Consistent with previous results, U5L-3′ RNA increased 1.9 ± 0.4-fold in the *sen1-K128E* single mutant. No significant increase was observed in the *mtr4-1* single mutant. In the double mutant, U5L-3′ RNA accumulation increased 2.1 ± 0.3-fold, which was statistically the same as that observed in the *sen1-K128E* single mutant. No significant effects on the accumulation of RNAs in the 271–960 nucleotide size range were observed in either the single or the double mutants.

Overall, the results reveal a synthetic interaction between *sen1-K128E* and *rrp6*Δ that is related to RNA processing and unrelated to transcription termination, suggesting that the Sen1p–Rnt1p protein–protein interaction may serve a role in promoting TRAMP-independent exosomal processing of the Rnt1p cleavage product. If this model is correct, then *sen1-K128E* should have no effect on the expression of U5 RNA when *RNT1* is deleted or when U5 RNA is altered by nucleotide substitutions that prevent Rnt1p recognition of the stem-loop in which Rnt1p cleaves. To test this, an allele of *SNR7* was created in which four nucleotides, AGUC, at the top of the Rnt1p recognition loop, were changed to GAAA (U5mt, Figure 4A). It was shown previously that this alteration prevents Rnt1p cleavage (Chanfreau *et al.* 2000). The wild-type and mutant versions of *SNR7* were expressed from plasmids in a strain carrying the wild-type *SNR7* gene. Due to overexpression, the mutant *snr7* RNAs outnumber the wild-type RNAs in strains producing U5mt from the plasmid.

The effects of *sen1-K128E* on the accumulation of the readthrough transcript and on RNAs in the 271–960 nucleotide size range were examined in strains carrying *rnt1*Δ or expressing cleavage-defective U5 RNA (U5mt) (Figure 5). The results indicate that *sen1-K128E* has no significant effect on either set of RNAs in *rnt1*Δ- or U5mt-expressing strains. The results suggest that the effects of *sen1-K128E* on *SNR7* expression are limited to exosomal processing of the immediate product of Rnt1p cleavage.

***SNR7* transcriptional readthrough increases expression of downstream *TOS2*:** Mutations in *SEN1* typically decrease the expression of downstream genes due to readthrough. For example, *sen1*-mediated readthrough of the small nucleolar RNA (snoRNA) gene *SNR13* reduces expression of the downstream gene, *TRS31* (Steinmetz and Brow 1996, 1998; Steinmetz *et al.* 2001, 2006). Since the *SNR7* readthrough transcripts end in the ORF of downstream *TOS2* (Figure 1E), we examined the effect of readthrough on *TOS2* expression.

In a *SEN1 RNT1* strain, *TOS2* mRNA was below the level of detection even when four times the standard 10 μg of RNA was loaded on the gel (Figure 6A). However, in a *sen1-1 rnt1*Δ strain, *TOS2* mRNA was readily detected, suggesting that the accumulation of U5-3′b RNA that occurs in *sen1-1 rnt1*Δ strains might cause increased expression of *TOS2*. To test this hypothesis, *TOS2* expression levels were compared by Northern blotting with a high specific activity riboprobe in a wild-type strain, a strain carrying a multi-copy *CUP1-TOS2* plasmid, and a strain carrying *sen1-1 rnt1*Δ (materials and methods; Figure 6B). *TOS2* was detected at a low level in the wild-type strain. *TOS2* mRNA expressed from the *CUP1-TOS2* plasmid was detected at levels comparable to the level observed in a *sen1-1 rnt1*Δ strain lacking the plasmid.

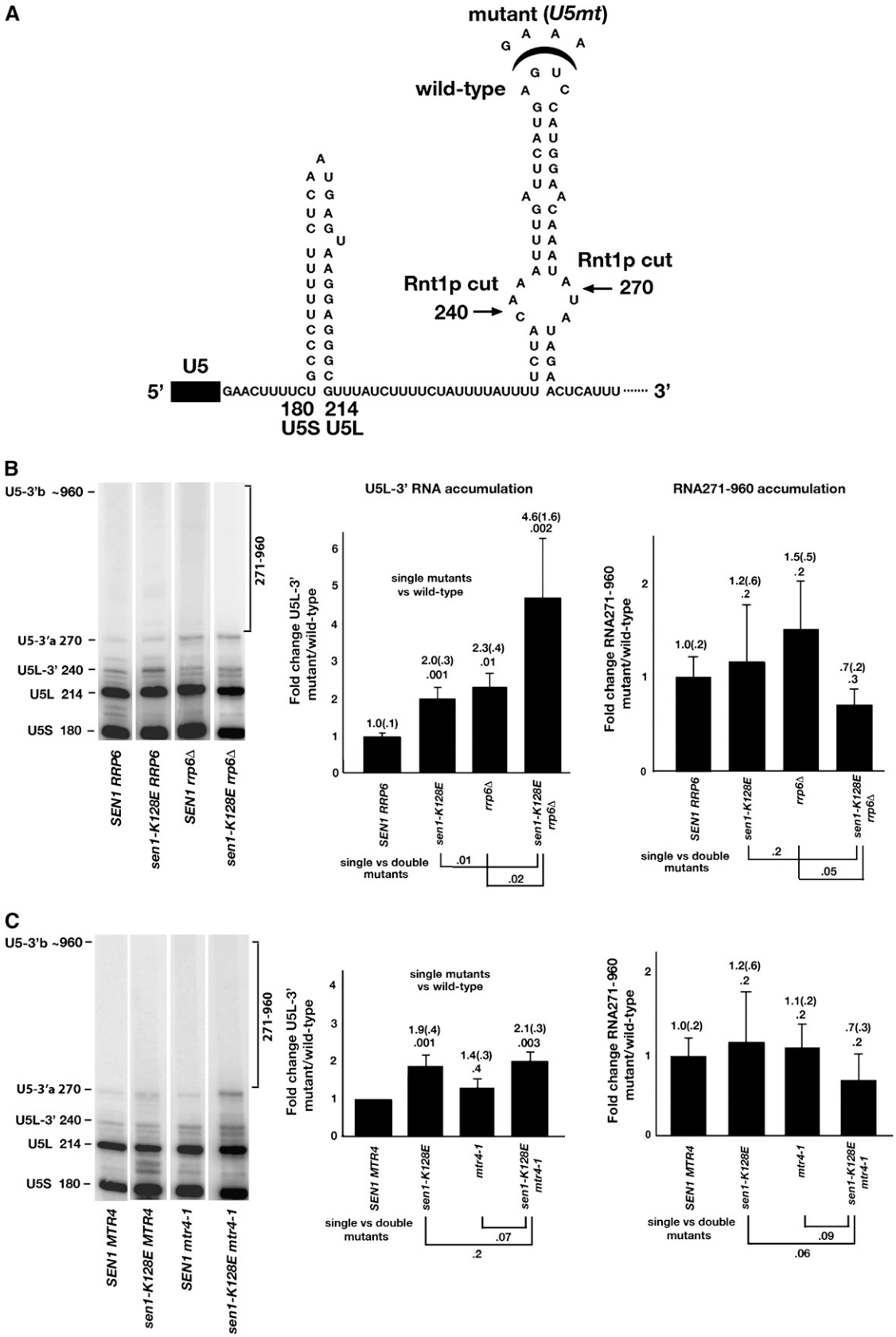


FIGURE 4.—Interactions between Sen1p with the exosomal nuclease Rrp6p and the TRAMP helicase Mtr4p. (A) Structure of the 3′ extended region of U5 RNA. Nucleotide substitution of AGUC in wild-type *SNR7* with GAAA at the top of the Rnt1p recognition stem-loop impairs the ability of Rnt1p to cleave the RNA (ELELA *et al.* 1996; CHANFREAU *et al.* 1997; LAMONTAGNE *et al.* 2000). (B) The representative Northern blots and bar graphs show the effects of *sen1-K128E* and *rrp6*Δ alone and in combination on the

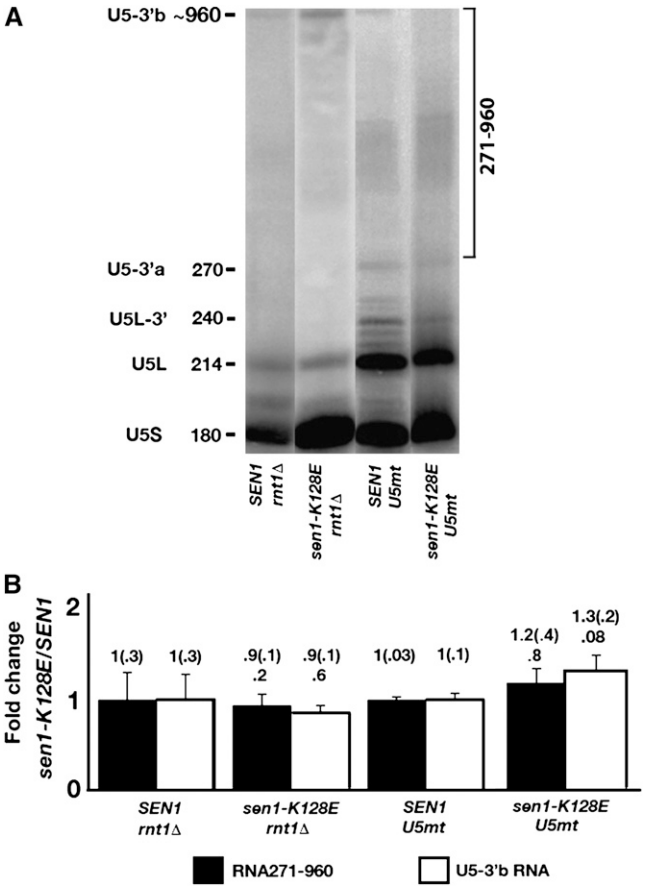


FIGURE 5.—Effects of *sen1-K128E* on *SNR7* expression in Rnt1p cleavage-defective strains. (A) RNA from strains carrying *SEN1* or *sen1-K128E* and either *rnt1*Δ or a plasmid expressing U5mt were analyzed by Northern blotting using the probe described in Figure 1B. A representative Northern blot is shown (see Figure 1 legend and MATERIALS AND METHODS). (B) The bar graph compares the effects on the accumulation of U5-3′b RNA and the sum of RNAs in the 271–960 size range (RNA271–960). Relative accumulation was quantitated as described in MATERIALS AND METHODS. Fold changes are indicated with the standard error in parentheses. *P*-values are indicated below the fold changes.

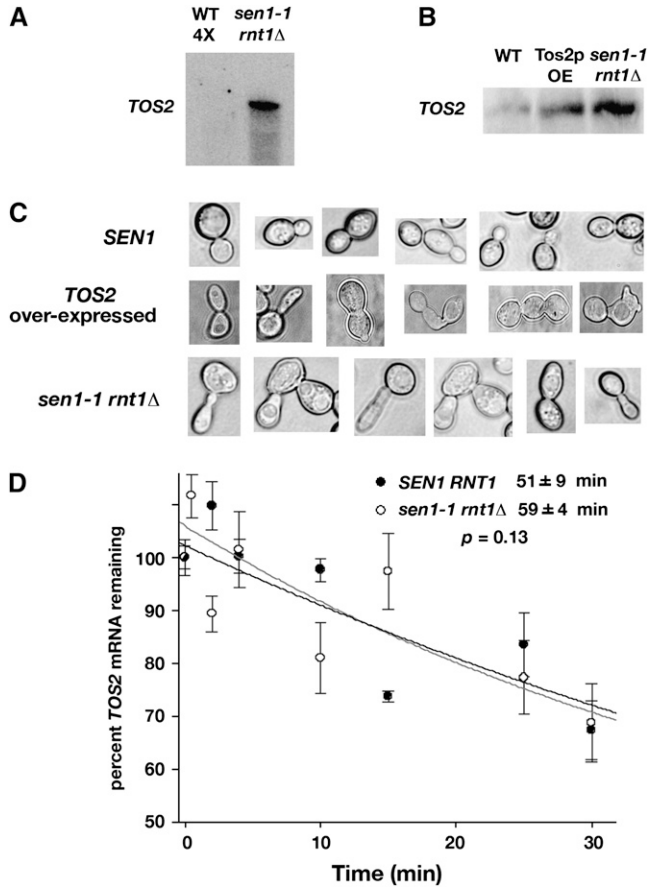


FIGURE 6.—Effect of *SNR7* transcriptional readthrough on expression of a downstream gene. (A) Increased expression of *TOS2* mRNA in a *sen1-1 rnt1*Δ strain. RNA levels were examined by Northern blotting using an end-labeled probe that anneals to the *TOS2* 3′-end. (B) *TOS2* RNA levels compared with overexpression of *CUP1-TOS2* from a multi-copy plasmid (designated Tos2p OE). RNA levels were examined by Northern blotting using a riboprobe (MATERIALS AND METHODS). (C) Cellular morphology of a strain that overexpresses *CUP1-TOS2* from a multi-copy plasmid and a strain that carries *sen1-1 rnt1*Δ. (D) Half-life of *TOS2* mRNA in *SEN1* and *sen1-1 rnt1*Δ strains.

Overexpression of *TOS2* from a multi-copy plasmid disrupts cytokinesis, leading to aberrant cell morphology, including multiple elongated buds (GANDHI *et al.* 2006). When the cell morphology of a wild-type strain was compared to that of a strain expressing *CUP1-TOS2* from a multi-copy plasmid and a strain carrying *sen1-1 rnt1*Δ, the elongated, multi-bud morphology was observed for the latter two strains compared to wild type (Figure 6C). Collectively, these results suggest that readthrough causes increased expression of *TOS2*.

*TOS2* mRNA levels might be elevated in *sen1-1 rnt1*Δ strains as the result of an increased rate of *TOS2* transcription or a decreased rate of mRNA decay. To distinguish between these models, the half-life of *TOS2* mRNA was determined. Transcription was inhibited with 10 μg/ml thiolutin. Northern blotting with a *TOS2*-specific end-labeled probe was used to monitor the disappearance of the preexisting mRNA at time intervals following inhibition (Figure 6D). The half-life of *TOS2* mRNA in a wild-type strain is 51 ± 9 min, which

relative accumulation of U5L-3′ RNA and the sum of RNAs in the 271–960 nucleotides size range (RNA271–960). (C) The Northern blots and bar graphs show the effects of *sen1-K128E* and *mtr4-1* alone and in combination on RNA accumulation as described in B. Relative accumulation was quantitated as described in MATERIALS AND METHODS. Fold changes are indicated with the standard error in parentheses. *P*-values are indicated below the fold changes. The brackets and numbers below the bar graphs indicate the *P*-values for single *vs.* double mutants.

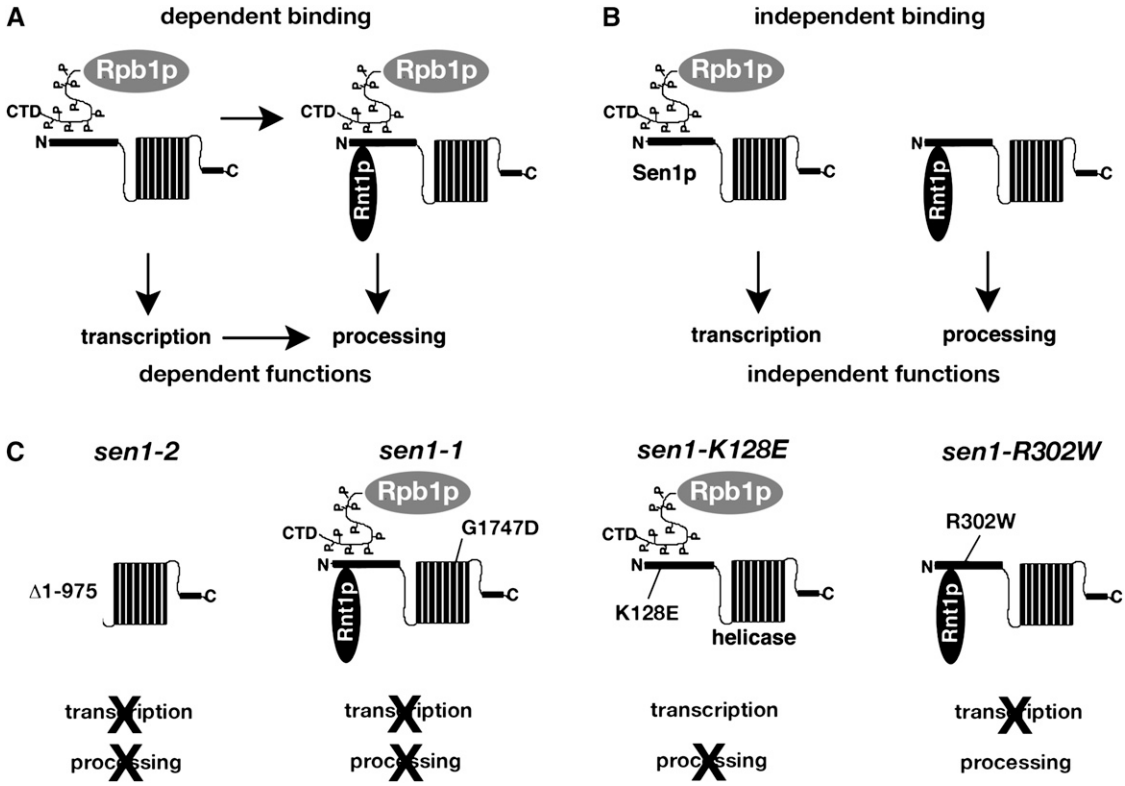


FIGURE 7.—Protein–protein interactions and their relationships to function. (A and B) Summaries of models for the relationship between the binding of Rpb1p and Rnt1p to Sen1p and the corresponding functional roles for Sen1p in transcription and processing. Sen1p, which binds to the C-terminal domain of Rpb1p (URSIC *et al.* 2004), is depicted as a helicase domain composed of stacked α-helices and an N-terminal segment containing multiple protein-binding domains. (C) Relationship between protein–protein interactions and function based on the phenotypes of *sen1* mutants.

is statistically indistinguishable from the 59 ± 4 min ($P = 0.13$) observed in the *sen1-1 rnt1*Δ strain. This indicates that readthrough has no effect on the stability of *TOS2* mRNA.

One way that *TOS2* expression might be elevated is through positive auto-regulation mediated by Tos2p itself. To test this model, pJF89, which expresses DNA including the *SNR7-TOS2* region but with *lacZ* replacing the *TOS2* ORF (MATERIALS AND METHODS), was transformed into strains carrying *SEN1* and *sen1-1*. β-Galactosidase assays revealed that the *sen1-1* strain had a 4.3 ± 2.3-fold increase in activity compared to wild type. Northern blotting revealed a 7.4 ± 1.8-fold increase in accumulation of the *lacZ* transcript in a *sen1-1* strain compared to wild type. These results indicate that increased expression is not dependent on the *TOS2* ORF and must therefore depend on upstream sequences.

## DISCUSSION

The goal of this study was to assess whether a genetic approach could be used to distinguish between alternative models for the functional relationships between protein–protein interactions. According to one model, interactions could occur in a dependent sequence of protein–protein binding reactions (Figure 7A). One way in which this could be achieved is if two binding domains overlap such that occupation of the domain for one protein precludes occupation by a second protein. Alternatively, protein–protein interactions might occur independently of each other, and there might be no obligate order of binding (Figure 7B). For a protein that interacts with multiple partners, coexistence of dependent and independent sets of binding reactions is possible.

To determine whether the Sen1p–Rnt1p and Sen1p–Rpb1p interactions depend on each other, we asked how they affect the function of Sen1p in the expression of *SNR7* coding for U5 snRNA. Two previously described alleles, *sen1-1*, which contains a point mutation in a conserved helicase motif, and *sen1-2*, which is missing DNA coding for the first 975 amino acids (URSIC *et al.* 2004), each cause two defects in *SNR7* expression: one in transcription termination and the other in 3′-end processing. Two new alleles described in this study, *sen1-K128E* and *sen1-R302W*, specifically impair the interactions with Rnt1p and Rpb1p, respectively. The mutants served as primary tools for asking how the termination and processing defects might be related. As summarized in Figure 7C, *sen1-K128E* caused elevated accumulation of the U5L-3′ RNA without detectable accumulation of

the readthrough RNA, whereas *sen1-R302W* caused accumulation of the readthrough RNA without excess accumulation of U5L-3′ RNA. The evidence supports a model for independent binding and independent function in transcription and processing since the phenotypic effects of mutations are genetically separable (Figure 7B).

It is likely that the defect in *SNR7* expression caused by *sen1-K128E* is entirely related to impaired Sen1p–Rnt1p binding because *sen1-K128E* had no phenotypic effects on RNA accumulation when the *RNT1* gene was deleted or when *SNR7* RNA was altered to a form that is immune to Rnt1p cleavage. On the basis of this and the synthetic effect of a *sen1-K128E rrp6*Δ exosome-defective double mutant on U5L-3′ RNA accumulation, we suggest that the primary purpose of the Sen1p–Rnt1p interaction is to assist the exosome in the processive shortening of U5L-3′ RNA to mature U5L by the exosome. The binding of Sen1p to Rnt1p might place Sen1p in physical proximity to the 3′-end of the exosomal substrate. The interaction could play a similar role in the processing of other noncoding RNAs that depend on Sen1p, Rnt1p, and the exosome.

Sen1p is a 5′–3′ helicase (Kim *et al.* 1999), whereas Mtr4p, a component of TRAMP that assists in exosomal degradation, is a 3′–5′ helicase (Liang *et al.* 1996; Lacava *et al.* 2005; Milligan *et al.* 2005). No synthetic interaction was observed in *sen1-K128E mtr4-1* double mutants. We propose that Mtr4p helicase activity is sufficient to aid the exosome in degrading most RNA structures. However, following Rnt1p cleavage, the RNA products may remain based-paired in the stem-loop region of the Rnt1p-binding/cleavage domain. Because of this, the 5′–3′ helicase activity of Sen1p may promote unwinding of the stem to force separation of the cleaved RNAs, allowing for efficient 3′ access to the exosome. Sen1p could assist the exosome in other regions of the RNA by providing a 5′–3′ unwinding activity, but it is not likely that this would depend on the Sen1p–Rnt1p protein–protein interaction.

The Sen1p–Rnt1p interaction may play a role in other RNA biosynthetic pathways in addition to U5 snRNA. We observed that both *sen1* and *rnt1* mutations cause changes in the accumulation of RNAs detected with probes complementary to the snoRNAs *SNR40* and *SNR47*. Furthermore, *sen1 rnt1* double mutants exhibited novel patterns of accumulation for *SNR40*- and *SNR47*-related RNAs (J. S. Finkel, unpublished observations), suggesting a potential role for the Sen1p–Rnt1p interaction in these pathways. However, other snoRNAs such as *SNR13* and *SNR10* were affected only by *sen1* mutations, and the effects are most likely restricted to defects in transcription termination (Steinmetz and Brow 1996, 1998; Rasmussen and Culbertson 1998; Steinmetz *et al.* 2001, 2006; Ursic *et al.* 2004).

It seemed possible that all functional roles for Sen1p during the transcription cycle might depend on the binding of Sen1p to the RNAP II subunit Rpb1p. Our genetic evidence argues against this model. Strains carrying *sen1-R302W* produce a protein that fails to bind to Rpb1p, but there is no observable defect in the processing of U5L-3′ RNA. Thus, despite the fact that transcription and processing are temporally coupled, the genetic data indicate that coupling is not enforced by a dependent sequence of protein–protein interactions. This does not necessarily mean that dependent sequences do not exist. Although it has not yet been tested, the interactions of Sen1p with Rpb1p and Rad2p (Ursic *et al.* 2004) could form a dependent sequence in which transcription-coupled DNA repair might require binding to Rpb1p as a prerequisite to Sen1p–Rad2p binding. The protein–protein interaction network in which Sen1p is embedded could be composed of sets of proteins that form both dependent and independent interactional and functional relationships. The broader possibilities remain to be tested.

The binding of Sen1p to Rpb1p is required for termination of transcription of the *SNR7* gene, since *sen1-R302W* causes accumulation of a readthrough transcript that extends into the downstream *TOS2* gene. Similar effects of *sen1* mutants on transcriptional termination have been reported for many other noncoding RNA genes (Steinmetz and Brow 1996, 1998; Rasmussen and Culbertson 1998; Steinmetz *et al.* 2001). What distinguishes the readthrough effect for *SNR7* is that the extended transcript causes increased rather than decreased expression of *TOS2*.

Typically, the expectation is that promoter occlusion would decrease expression of the downstream gene. We ruled out the possibility that increased expression is mediated at the level of mRNA stability or by Tos2p-mediated auto-regulation because there was no effect on the *TOS2* mRNA half-life and because increased expression was observed when the *TOS2* ORF was replaced with the *lacZ* ORF. Since increased expression must involve sequences upstream of the *TOS2* ORF, an elevated rate of *TOS2* transcription is likely. One way this could occur is if the readthrough transcript displaces a transcriptional repressor. Such displacement could override the potential effects of promoter occlusion, leading to a net increase in transcription.

This research was supported by the University of Wisconsin College of Agricultural and Life Sciences, the School of Medicine and Public Health, National Institutes of Health grant GM65172 (M.R.C.), National Science Foundation grant MCB 0744017 (M.R.C.), and Kirschstein National Research Service Award Individual predoctoral fellowship F31 GM077078 (J.S.F.). This is Laboratory of Genetics paper no. 3645.

## LITERATURE CITED

Allmang, C., J. Kufel, G. Chanfreau, P. Mitchell, E. Petfalski *et al.*, 1999 Functions of the exosome in rRNA, snoRNA and snRNA synthesis. EMBO J. **18:** 5399–5410.

Boeke, J. D., F. LaCroute and G. R. Fink, 1984 A positive selection for mutants lacking orotidine-5′-phosphate decarboxylase activity

in yeast: 5-fluoro-orotic acid resistance. Mol. Gen. Genet. **197:** 345–346.

Chanfreau, G., S. A. Elela, M. Ares, Jr. and C. Guthrie, 1997 Alternative 3′-end processing of U5 snRNA by RNase III. Genes Dev. **11:** 2741–2751.

Chanfreau, G., P. Legrain and A. Jacquier, 1998 Yeast RNase III as a key processing enzyme in small nucleolar RNAs metabolism. J. Mol. Biol. **284:** 975–988.

Chanfreau, G., M. Buckle and A. Jacquier, 2000 Recognition of a conserved class of RNA tetraloops by Saccharomyces cerevisiae RNase III. Proc. Natl. Acad. Sci. USA **97:** 3142–3147.

Chen, Y. Z., C. L. Bennett, H. M. Huynh, I. P. Blair, I. Puls *et al.*, 2004 DNA/RNA helicase gene mutations in a form of juvenile amyotrophic lateral sclerosis (ALS4). Am. J. Hum. Genet. **74:** 1128–1135.

Chen, Y. Z., S. H. Hashemi, S. K. Anderson, Y. Huang, M. C. Moreira *et al.*, 2006 Senataxin, the yeast Sen1p orthologue: characterization of a unique protein in which recessive mutations cause ataxia and dominant mutations cause motor neuron disease. Neurobiol. Dis. **23:** 97–108.

Conrad, N. K., S. M. Wilson, E. J. Steinmetz, M. Patturajan, D. A. Brow *et al.*, 2000 A yeast heterogeneous nuclear ribonucleoprotein complex associated with RNA polymerase II. Genetics **154:** 557–571.

DeMarini, D. J., M. Winey, D. Ursic, F. Webb and M. R. Culbertson, 1992 SEN1, a positive effector of tRNA-splicing endonuclease in *Saccharomyces cerevisiae*. Mol. Cell. Biol. **12:** 2154–2164.

Duquette, A., K. Roddier, J. McNabb-Baltar, I. Gosselin, A. St-Denis *et al.*, 2005 Mutations in senataxin responsible for Quebec cluster of ataxia with neuropathy. Ann. Neurol. **57:** 408–414.

Elela, S. A., H. Igel and M. Ares, Jr., 1996 RNase III cleaves eukaryotic preribosomal RNA at a U3 snoRNP-dependent site. Cell **85:** 115–124.

Fromont-Racine, M., J. C. Rain and P. Legrain, 1997 Toward a functional analysis of the yeast genome through exhaustive two-hybrid screens. Nat. Genet. **16:** 277–282.

Gandhi, M., B. L. Goode and C. S. Chan, 2006 Four novel suppressors of *gic1 gic2* and their roles in cytokinesis and polarized cell growth in *Saccharomyces cerevisiae*. Genetics **174:** 665–678.

Gietz, R. D., and R. A. Woods, 2002 Transformation of yeast by the Liac/SS carrier DNA/PEG method. Methods Enzymol. **350:** 87–96.

Grigoriev, A., 2003 On the number of protein-protein interactions in the yeast proteome. Nucleic Acids Res. **31:** 4157–4161.

Guan, Q., W. Zheng, S. Tang, X. Liu, R. A. Zinkel *et al.*, 2006 Impact of nonsense-mediated mRNA decay on the global expression profile of budding yeast. PLoS Genet. **2:** 1924–1943.

Habraken, Y., P. Sung, L. Prakash and S. Prakash, 1993 Yeast excision repair gene *RAD2* encodes a single-stranded DNA endonuclease. Nature **366:** 365–368.

Hanawalt, P. C., and G. Spivak, 2008 Transcription-coupled DNA repair: two decades of progress and surprises. Nat. Rev. Mol. Cell Biol. **9:** 958–970.

Kambach, C., S. Walke, R. Young, J. M. Avis, E. de la Fortelle *et al.*, 1999 Crystal structures of two Sm protein complexes and their implications for the assembly of the spliceosomal snRNPs. Cell **96:** 375–387.

Kim, H. D., J. Choe and Y. S. Seo, 1999 The sen1(+) gene of Schizosaccharomyces pombe, a homologue of budding yeast SEN1, encodes an RNA and DNA helicase. Biochemistry **38:** 14697–14710.

Komarnitsky, P., E. J. Cho and S. Buratowski, 2000 Different phosphorylated forms of RNA polymerase II and associated mRNA processing factors during transcription. Genes Dev. **14:** 2452–2460.

LaCava, J., J. Houseley, C. Saveanu, E. Petfalski, E. Thompson *et al.*, 2005 RNA degradation by the exosome is promoted by a nuclear polyadenylation complex. Cell **121:** 713–724.

Lamontagne, B., A. Tremblay and S. Abou Elela, 2000 The N-terminal domain that distinguishes yeast from bacterial RNase III contains a dimerization signal required for efficient double-stranded RNA cleavage. Mol. Cell. Biol. **20:** 1104–1115.

Liang, S., M. Hitomi, Y. H. Hu, Y. Liu and A. M. Tartakoff, 1996 A DEAD-box-family protein is required for nucleocytoplasmic transport of yeast mRNA. Mol. Cell. Biol. **16:** 5139–5146.

Maniatis, T., and R. Reed, 2002 An extensive network of coupling among gene expression machines. Nature **416:** 499–506.

Milligan, L., C. Torchet, C. Allmang, T. Shipman and D. Tollervey, 2005 A nuclear surveillance pathway for mRNAs with defective polyadenylation. Mol. Cell. Biol. **25:** 9996–10004.

Moreira, M. C., S. Klur, M. Watanabe, A. H. Nemeth, I. Le Ber *et al.*, 2004 Senataxin, the ortholog of a yeast RNA helicase, is mutant in ataxia-ocular apraxia 2. Nat. Genet. **36:** 225–227.

Myer, V. E., and R. A. Young, 1998 RNA polymerase II holoenzymes and subcomplexes. J. Biol. Chem. **273:** 27757–27760.

Nedea, E., D. Nalbant, D. Xia, N. T. Theoharis, B. Suter *et al.*, 2008 The Glc7 phosphatase subunit of the cleavage and polyadenylation factor is essential for transcription termination on snoRNA genes. Mol. Cell **29:** 577–587.

Neugebauer, K. M., 2002 On the importance of being co-transcriptional. J. Cell Sci. **115:** 3865–3871.

Patterson, B., and C. Guthrie, 1987 An essential yeast snRNA with a U5-like domain is required for splicing in vivo. Cell **5:** 613–624.

Prakash, S., and L. Prakash, 2000 Nucleotide excision repair in yeast. Mutat. Res. **451:** 13–24.

Rasmussen, T. P., and M. R. Culbertson, 1998 The putative nucleic acid helicase Sen1p is required for formation and stability of termini and for maximal rates of synthesis and levels of accumulation of small nucleolar RNAs in Saccharomyces cerevisiae. Mol. Cell. Biol. **18:** 6885–6896.

Roy, J., B. Zheng, B. C. Rymond and J. L. Woolford, Jr., 1995 Structurally related but functionally distinct yeast SmD core small nuclear ribonucleoprotein particle proteins. Mol. Cell. Biol. **15:** 445–455.

Stahl, G., L. Bidou, J. P. Rousset and M. Cassan, 1995 Versatile vectors to study recoding: conservation of rules between yeast and mammalian cells. Nucleic Acids Res. **23:** 1557–1560.

Steinmetz, E. J., and D. A. Brow, 1996 Repression of gene expression by an exogenous sequence element acting in concert with a heterogeneous nuclear ribonucleoprotein-like protein, Nrd1, and the putative helicase Sen1. Mol. Cell. Biol. **16:** 6993–7003.

Steinmetz, E. J., and D. A. Brow, 1998 Control of pre-mRNA accumulation by the essential yeast protein Nrd1 requires high-affinity transcript binding and a domain implicated in RNA polymerase II association. Proc. Natl. Acad. Sci. USA **95:** 6699–6704.

Steinmetz, E. J., N. K. Conrad, D. A. Brow and J. L. Corden, 2001 RNA-binding protein Nrd1 directs poly(A)-independent 3′-end formation of RNA polymerase II transcripts. Nature **413:** 327–331.

Steinmetz, E. J., S. B. Ng, J. P. Cloute and D. A. Brow, 2006 Cis- and trans-Acting determinants of transcription termination by yeast RNA polymerase II. Mol. Cell. Biol. **26:** 2688–2696.

Suraweera, A., O. J. Becherel, P. Chen, N. Rundle, R. Woods *et al.*, 2007 Senataxin, defective in ataxia oculomotor apraxia type 2, is involved in the defense against oxidative DNA damage. J. Cell Biol. **177:** 969–979.

Suraweera, A., Y. Lim, R. Woods, G. W. Birrell, T. Nasim *et al.*, 2009 Functional role for senataxin, defective in ataxia oculomotor apraxia type 2, in transcriptional regulation. Hum. Mol. Genet. **18:** 3384–3396.

Ursic, D., K. Chinchilla, J. S. Finkel and M. R. Culbertson, 2004 Multiple protein/protein and protein/RNA interactions suggest roles for yeast DNA/RNA helicase Sen1p in transcription, transcription-coupled DNA repair and RNA processing. Nucleic Acids Res. **32:** 2441–2452.

Wach, A., A. Brachat, R. Pöhlmann and P. Philippsen, 1994 New heterologous modules for classical or PCR-based gene disruptions in *Saccharomyces cerevisiae*. Yeast **10:** 1793–1808.

Zhang, D., N. Abovich and M. Rosbash, 2001 A biochemical function for the Sm complex. Mol. Cell **7:** 319–329.

Communicating editor: M. Hampsey